Self-Assembling Light Harvesting Systems From Synthetically Modified Tobacco Mosaic Virus Coat Protein

Rebekah A. Miller, Andrew D. Presley, and Matthew B. Francis*

Department of Chemistry, University of California, Berkeley, CA 94720-1460, and Material Science Division, Lawrence Berkeley National Labs, Berkeley, CA 94720-1460

Supporting Information and Figures

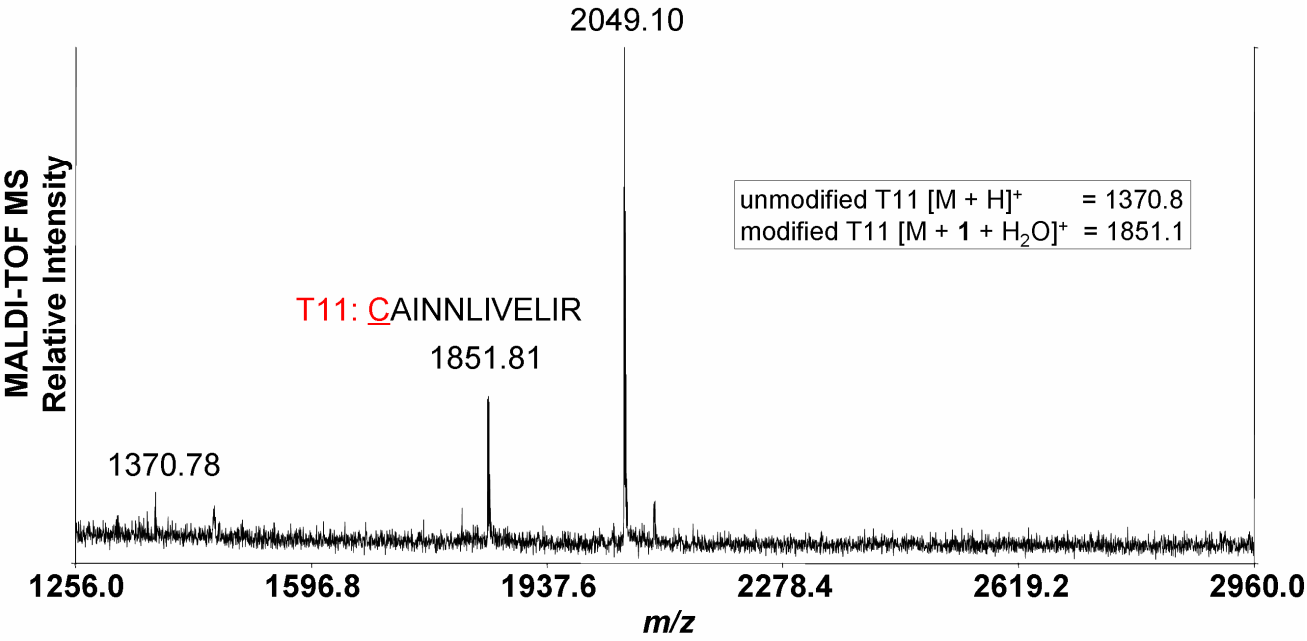

Supporting Information Figure S1: MALDI-TOF MS analysis of modified TMVP trypsin digest. Native T11 fragment containing C123, expected *m/z* = 1370.8; T11 fragment modified with one Oregon Green maleimide and one water molecule, expected *m/z* = 1851.8; native T6 fragment used for mass calibration, *m/z* = 2049.1.

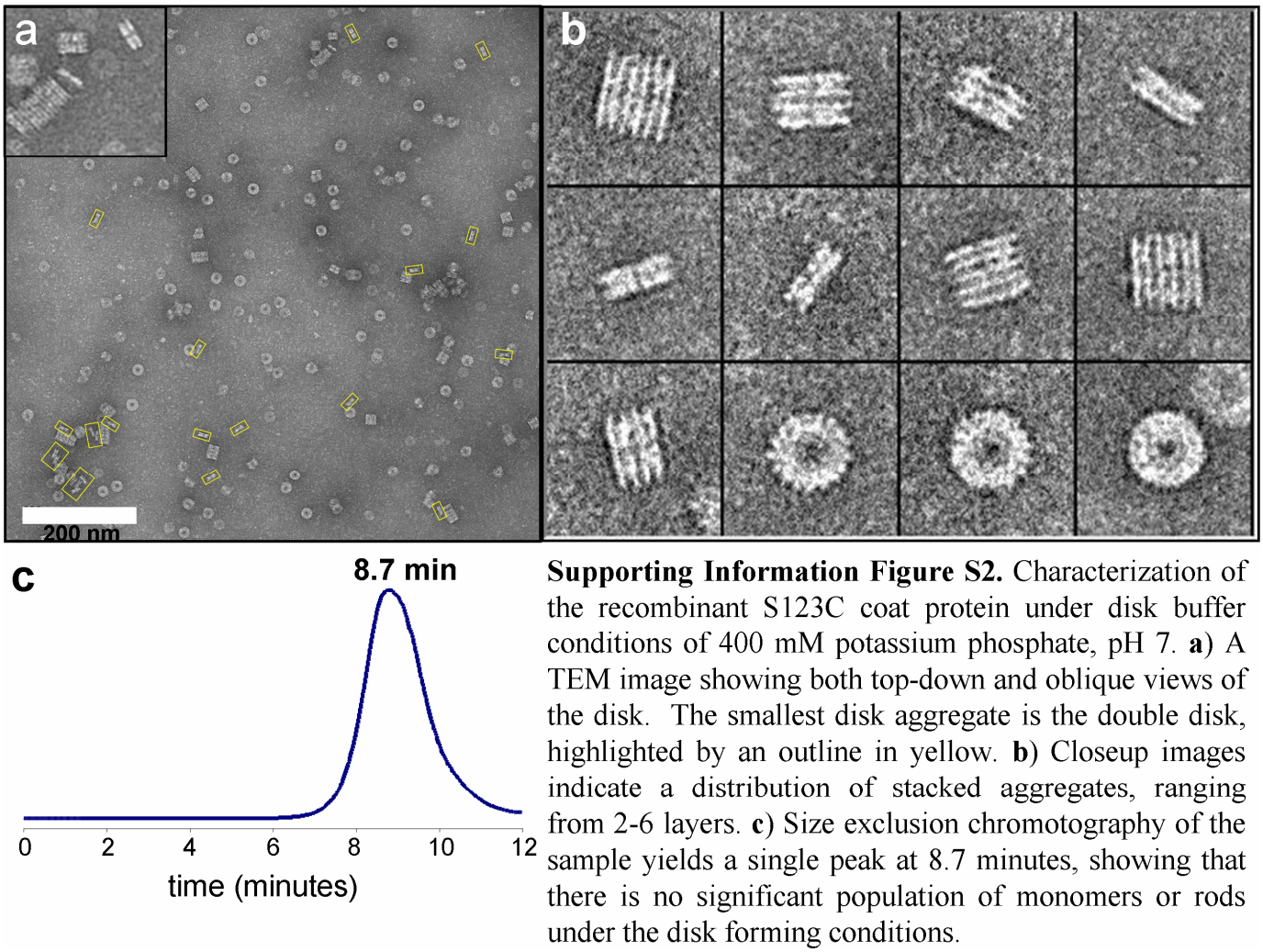

Supporting Information Figure S2. Characterization of the recombinant S123C coat protein under disk buffer conditions of 400 mM potassium phosphate, pH 7. **a**) A TEM image showing both top-down and oblique views of the disk. The smallest disk aggregate is the double disk, highlighted by an outline in yellow. **b**) Closeup images indicate a distribution of stacked aggregates, ranging from 2-6 layers. **c**) Size exclusion chromotography of the sample yields a single peak at 8.7 minutes, showing that there is no significant population of monomers or rods under the disk forming conditions.

Energy transfer calculations. In order to estimate the Förster radius of chromophores displayed within TMVP rods, the relative fluorescence quantum yield of chromophore **1** was determined at rod conditions (100 sodium acetate, pH 5.5) by the method of Williams et al. (Supporting Information, Figure S3).[1] Fluorescein, with a quantum yield of 0.92 under buffer conditions of 50 mM phosphate buffer, pH 9.0, was used at a standard in these experiments. At rod buffer conditions, chromophore **1** was found to have a quantum yield of 0.17. Samples of increasing concentration (1 nM to 10 nM for fluorescein, and 10 nM to 100 nM for **1**) were excited at 495 nm and the integrated fluorescence emission (505 to 600 nm) was quantified. The integrated fluorescence intensity was plotted against the maximum absorbance of the sample, as extrapolated from absorbance measurements made of samples at 1000-fold higher concentrations. The data were fit by a linear trendline in Excel, incorporating a zero intercept. The slope, which is proportional to the quantum yield, was calculated using the fluorescein standard as follows:

$$\Phi_x = \Phi_{st}\left(\frac{m_x}{m_{st}}\right)\left(\frac{n^2{}_x}{n^2{}_{st}}\right)$$

where Φ_{st} represents the quantum yield of the standard, Φ_x represents the quantum yield of chromophore **1**, m_{st} represents the slope of the best linear fit for the standard plot, m_x represents the slope of the best linear fit for the chromophore **1** plot, and *n* is the refractive index of the buffer used. Since both buffers were aqueous, the refractive index ratio was approximated to be unity.

The spectral overlap integral was then calculated using the following equation[2]

$$J = \int_0^\infty f_D(\lambda)\varepsilon_A(\lambda)\lambda^4 d\lambda$$

where λ is the wavelength of light (nm), $\varepsilon_A(\lambda)$ is the molar absorbtivity of the acceptor at that wavelength (M^{-1} cm^{-1}), and $f_D(\lambda)$ is the donor fluorescence spectrum normalized on the wavelength scale such that

$$1 = \int_0^\infty f_D(\lambda)d\lambda$$

The overlap integral was found to be 2.4 x 10^{15} M^{-1} cm^{-1} nm^4 for transfer between chromophores **1** and **3**, and 1.4 x 10^{15} M^{-1} cm^{-1} nm^4 for transfer between two chromophore **1** molecules**.**

Assuming a value of 2/3 for the orientation value κ^2, an aqueous refractive index of $\eta = 1.33$, and leaving the overlap integral J in the units described above, the Förster radius can be calculated using the following equation:[3]

$$R_0(\text{Å}) = 0.211 \times \left(J\Phi\kappa^2 n^{-4}\right)^{1/6}$$

The Förster radius was thus estimated to be 4.0 nm for transfer between two molecules of chromophore **1**, and 4.4 nm for transfer between chromophores **1** and **3.**

The relative rates of the two paths of energy transfer outlined previously were then calculated (Figure S3). The rate of transfer is defined as:

$$k_T = \frac{J\kappa^2\lambda_d}{r^6 n^4} \times 8.71 \times 10^{23}\ \text{sec}^{-1}$$

where λ_d is the emissive rate of the donor and r is the distance between the two chromophores.[4] When determining the relative rate of transfer between chromophores in the same orientation, as should be observed for chromophores attached within the TMVP rod assembly, this equation simplifies. For example, when comparing the rate of transfer Path 2a (from OG_1 to OG_2) to that of Path 1 (from OG_1 to AF), the equation can be represented as follows (See Figure S3):

$$\frac{k_{T(OG_1OG_2)}}{k_{T(OG_2AF)}} = \left(\frac{r_{OG_1OG_2}}{r_{OG_1AF}}\right)^6 \frac{J_{OG_1AF}}{J_{OG_1OG_2}}$$

Employing this treatment, the relative rates of each step in the two paths outlined previously are tabulated in Figure S3. As the inverse of a rate constant has units of time, the relative durations of the two pathways can be compared in the following manner:

$$\frac{1}{k_{(Path1)}} \times x = \frac{1}{k_{(Path2a)}} + \frac{1}{k_{(Path2b)}}$$

Path 2 (including both steps **2a** and **2b**) was found to be 20 times faster than Path 1, suggesting that while direct energy transfer from nonadjacent donors certainly contributes to acceptor emission, degenerate donor-to-donor transfer steps can funnel energy into the acceptor occur much more quickly.

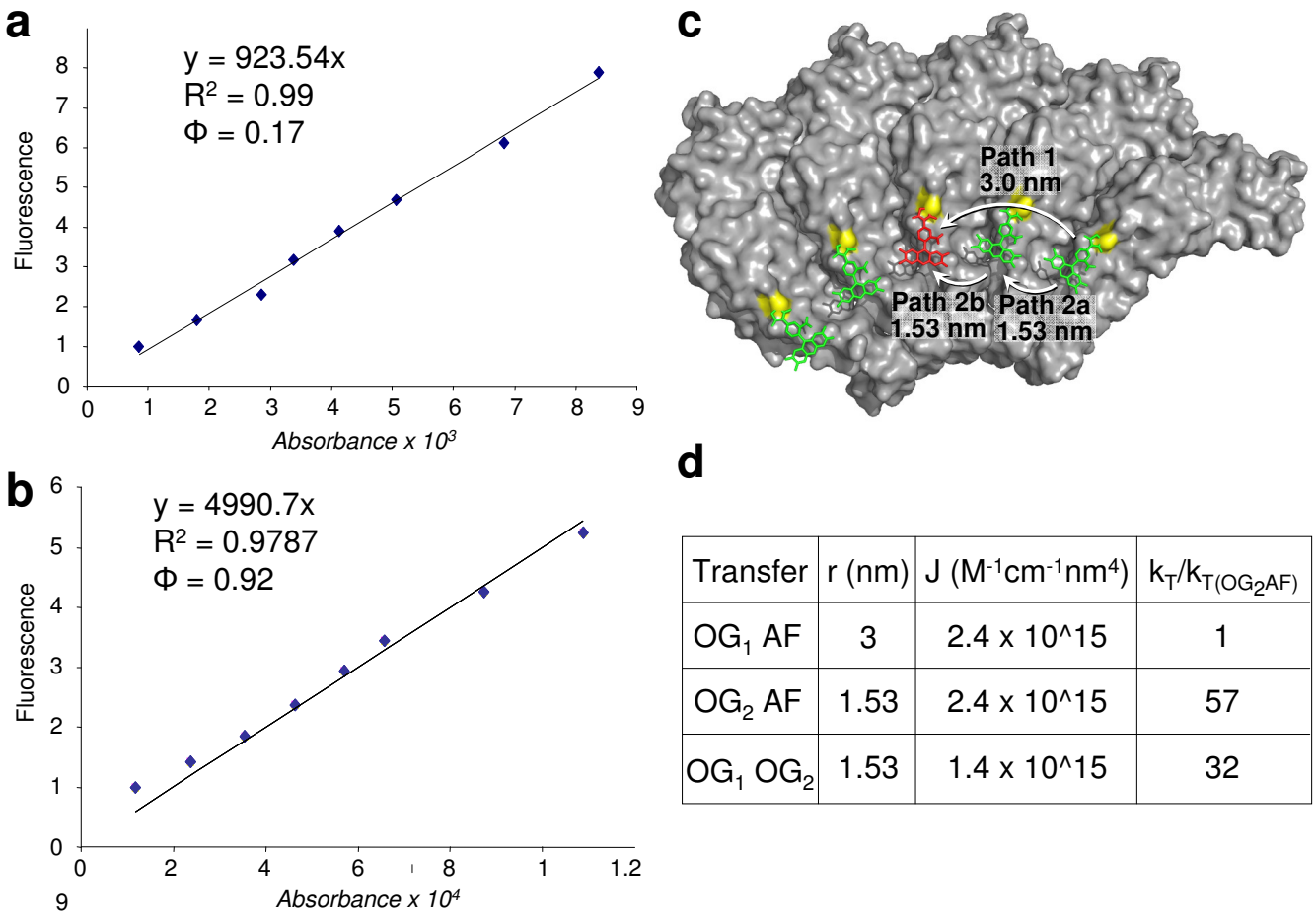

Transfer	r (nm)	J ($M^{-1}cm^{-1}nm^4$)	$k_T/k_{T(OG_2AF)}$
OG_1 AF	3	2.4 x 10^15	1
OG_2 AF	1.53	2.4 x 10^15	57
OG_1 OG_2	1.53	1.4 x 10^15	32

Supporting Information Figure S3. Energy transfer calculations for the two chromophore system. Fluorescence vs. absorbance plots used to determine the relative quantum yield of **a**) chromophore **1** in rod buffer and **b**) the reference standard, fluorescein. **c**) A schematic of two pathways by which a donor chromophore **1** can transfer energy to a nonadjacent acceptor chromophore **3**. Path 1 illustrates the direct transfer of energy from the nonadjacent donor (OG_1) to the acceptor (AF). Path 2 depicts a two-step process in which the nonadjacent donor chromophore first transfers energy to the intervening donor chromophore (OG_2), which in turn transfers energy to the acceptor. **d**) Tabulation of the parameters necessary for calculating the relative rates of each pathways. The distance between chromophores, r, was determined by measuring the shortest line between the center of each. Calculation of the overlap integral, J, is described in the text.

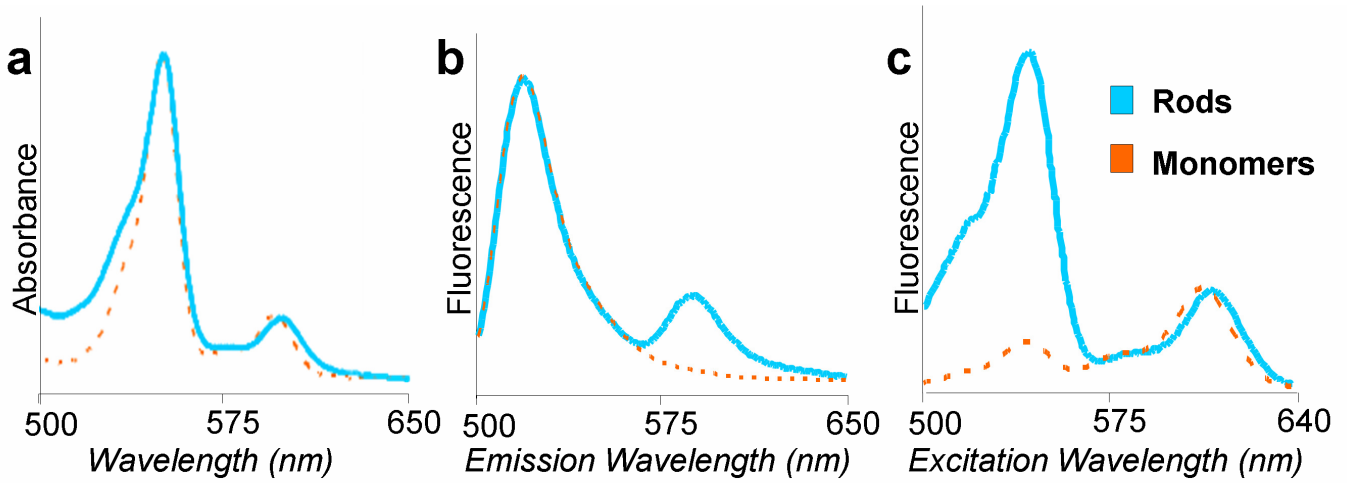

Supporting Information Figure S4: In systems containing a 16:1 ratio of donor **1** to acceptor **3,** efficient energy transfer requires assembly from monomers into rods. **a**) Absorbance spectra of monomers and rods show an identical ratio of **1** to **3**. **b**) Donor excitation (495 nm) results in acceptor emission (617 nm) for assembled rods. Monomers fluoresce only at the donor emission wavelength (520 nm). **c**) Excitation spectra (em = 650 nm) reveal that the donor chromophore contributes a significant amount of energy towards acceptor emission only in the rod assembly state.

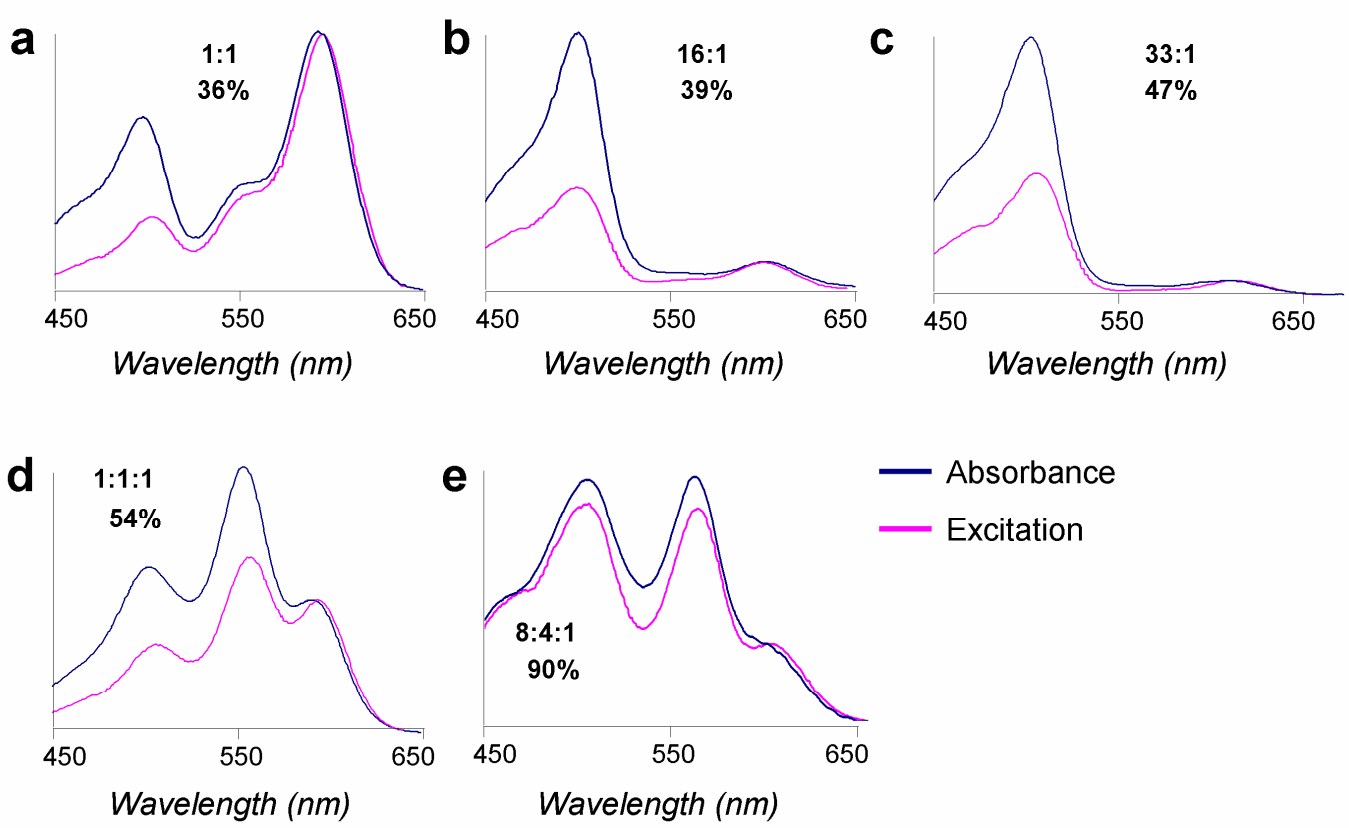

Supporting Information Figure S5: Overlays of the absorbance and excitation spectra of the two and three chromophore systems. In the two chromophore system (**a-c**), a maximum efficiency of 47% is observed in the 33:1 donor **1** to acceptor **3** system. The three dye system (**d-e**) achieves much higher efficiencies due to increased spectral overlap, with the 8:4:1 donor **1** : donor **2** : acceptor **3** system exhibiting over 90% efficiency in transferring energy from **1** to **3**.

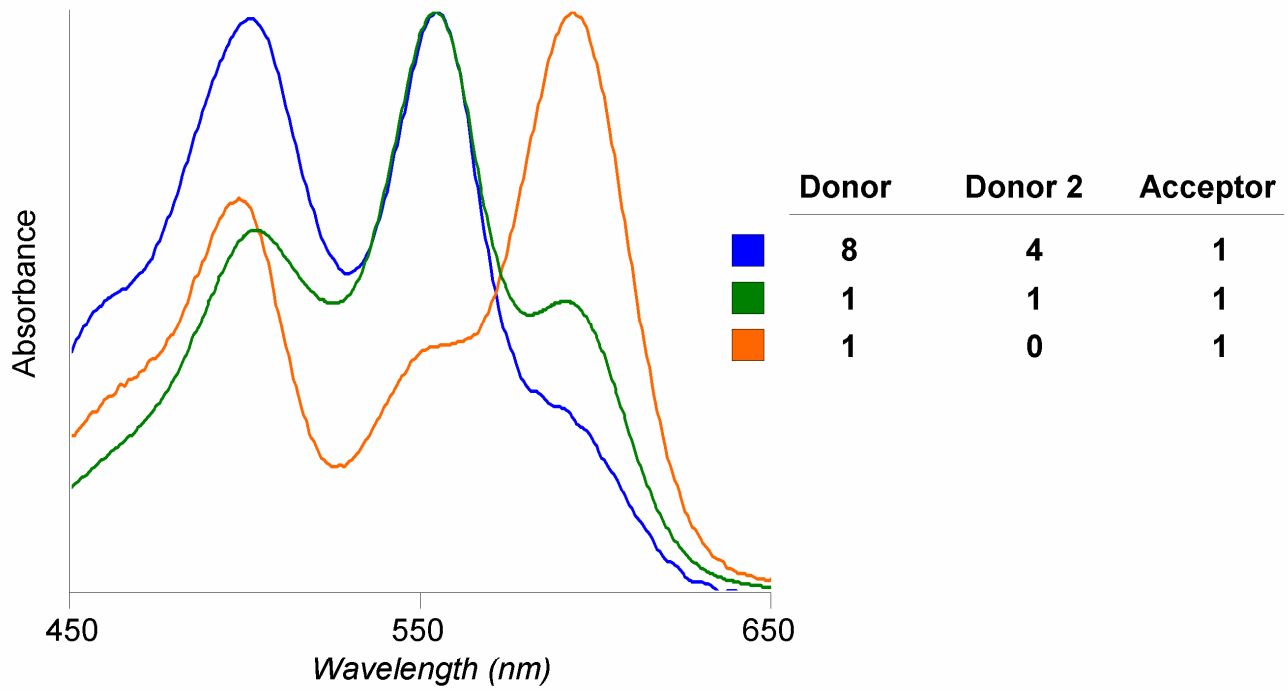

Supporting Information Figure S6: Absorbance spectra of rod assemblies containing various ratios of Donor **1**, Donor **2**, and Acceptor **3.** Spectra were collected in 100 mM acetate buffer, pH 5.5.

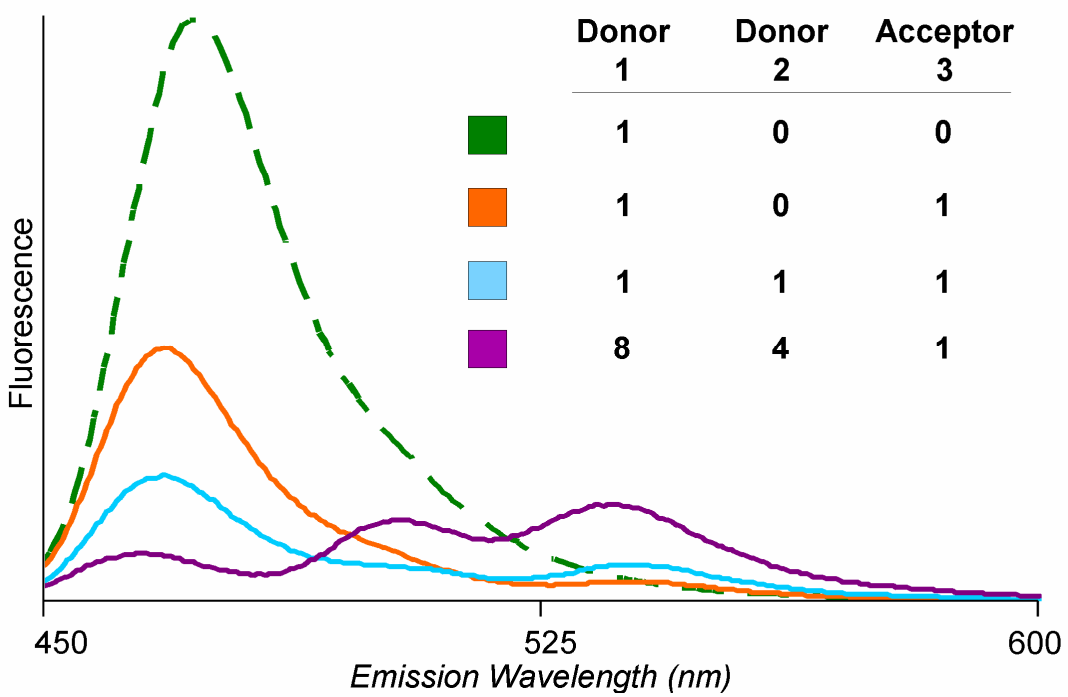

Supporting Information Figure S7: Overlay of the emission spectra of selected one, two and three chromophore systems. Efficiency is defined as the percent decrease in donor fluorescence compared to a system containing no acceptor dyes. Efficiency increases with increasing donor ratios and spectral overlap. Rods containing chromophores **1**, **2**, and **3** in a 8:4:1 ratio exhibit 92% quenching.

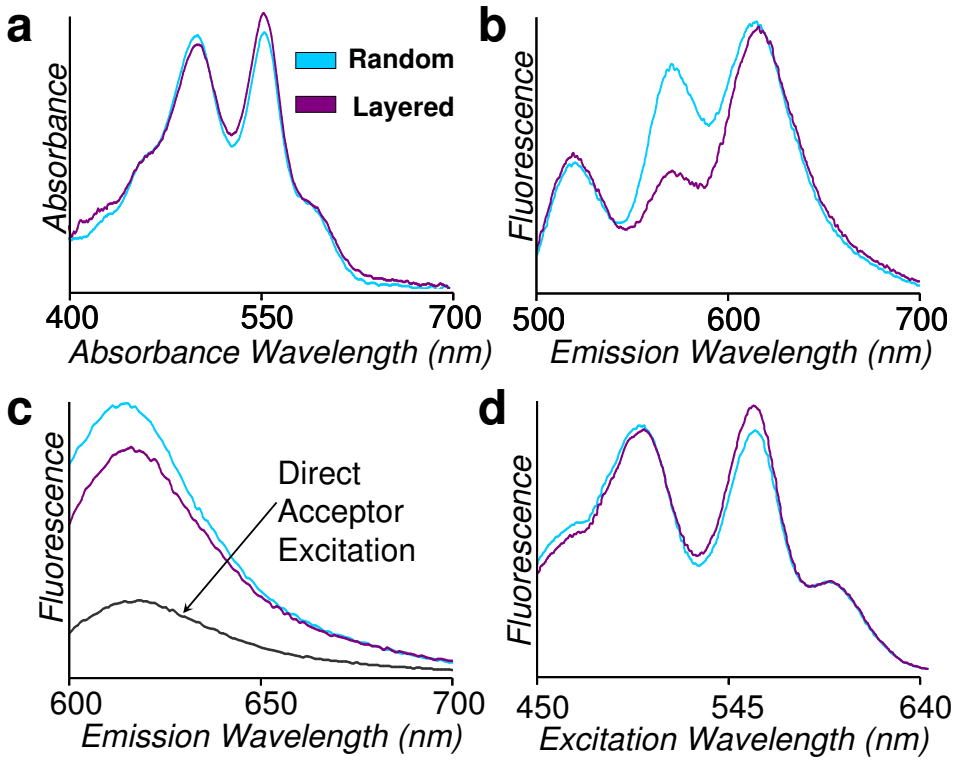

Supporting Information Figure S8: A comparison of rods containing chromophores **1**, **2**, and **3** in a 8:4:1 ratio, in which chromophores are either randomly distributed (purple) or layered through assembly from preformed disks (blue). **a**) Absorbance spectra (normalized at 495 nm) indicates an identical ratio of the three chromophores in each system. **b)** An emission spectra (normalized at 495 nm) reveals that donor **1** quenching occurs to a similar degree in each system. However, the layered system exhibits increased chromophore **2** emission (λ_{em} = 550 nm). **c)** The antenna effect is slightly greater for the system with layered chromophore distribution. Each spectrum is shown relative to the sample's acceptor emission (em = 617 nm) due to direct excitation (ex = 588 nm), shown in black. **d)** An overlay of the excitation wavelengths contributing to chromophore **3** emission (650 nm) suggests that energy transfer from chromophores **1** and **2** is largely independent of chromophore distribution.

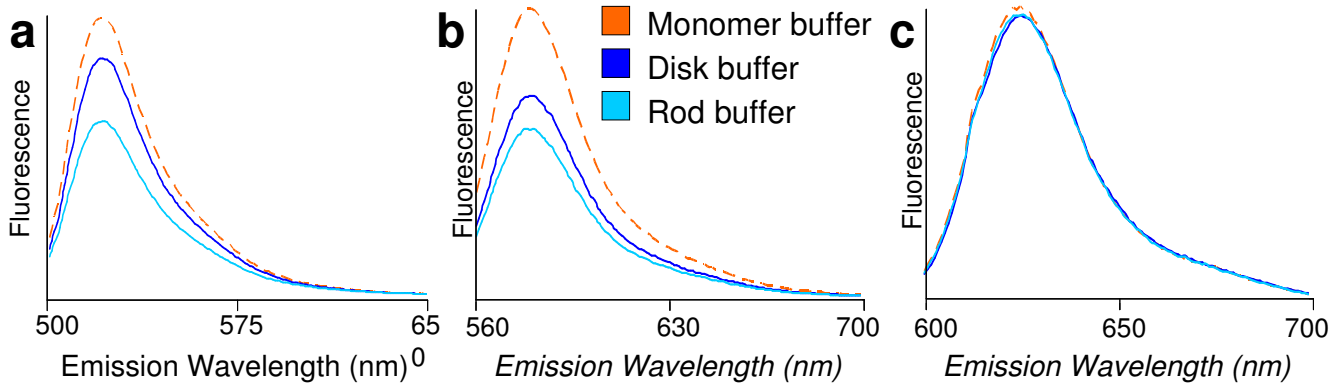

Supporting Information Figure 9: Emission spectra of **a**) Oregon Green 488, normalized to absorbance at 495 nm, **b**) Tetramethylrhodamine, normalized to absorbance at 550 nm, and **c**) Alexa Fluor 594, normalized to absorbance at 597nm in the monomer buffer (25 mM potassium phosphate, pH 8), disk buffer (400 mM potassium phosphate, pH 7.0), and rod buffer (100 mM sodium acetate, pH 5.5).

References for Supporting Information Section

[1] a) Mottram, L. F.; Boonyarattanakalin, S.; Kovel, R. E.; Peterson, B. R. *Org. Lett.* **2006**, *8*, 581-584. b) Williams, A. T.; Winfield, S.A. *Analyst* **1982**, 108, 1067-1071.

[2] a) Montali, A.; Harms, G. S.; Renn, A.; Weder, C.; Smith, P.; Wild, U. P. *Physical Phys. Chem. Chem. Phys.* **1999**, *1*, 5697-5702. b) Van Der Meer, B. W.; Coker, G.; Chen, S.-Y. *Resonance Energy Transfer*, VCH, New York, 1994.

[3] Lakowicz, J.R. Topics in Fluorescence Spectroscopy: Principles, Plenum Press, New York, 1991.

[4] Lakowicz, J.R. Principles of Fluorescence Spectroscopy, Plenum Press, New York, 1983.